HiSST: 2nd International Conference on
High-Speed Vehicle Science & Technology

16–19 May 2022, Bruges, Belgium

Surrogate modelling of supersonic fuel-air mixing in a multi-strut injection scramjet engine using artificial neural network

Ali Can Ispir [1], Kamila Zdybał [2], Bayindir H. Saracoglu [3], Thierry Magin [4], Axel Coussement [5]

Abstract

One of the main challenges which must be hurdled in the dual mode ramjet/scramjet engines' design process, is to obtain an optimal fuel-air mixing distribution and a good penetration. One way is to enhance the mixing efficiency is to inject the fuel via multiple struts in parallel direction and make the fuel be mixed with air throughout the shock-expansion waves structure. Mixing intensity is augmented by the turbulence level highly depends on the strut geometrical parameters, however, this enhancement in the mixing can bring about several detrimental effects on the aerodynamic features of the propulsion system such as increasing the losses on total pressure. Therefore, optimizing configurations of the fuel struts and resolving the interaction between the design variables are obligatory in order to yield best overall engine performance. The present study focuses on the investigation of the strut design parameters impacts on the fuel-air mixing and aerodynamic properties particularly efficiency, length and total pressure recovery factor. We solved compressible non-reactive RANS filtered governing equations on the 2D flow domain of a dual mode ramjet engine (operating in scramjet mode) combustor. Exploring the design space of the fuel struts in terms of mixing and total pressure losses, requires plenty of simulations and an informative dataset. Performing the simulations in every single design point is computationally prohibitively expensive. Machine learning techniques thus can be a key solution for multi-objective optimization of design variables, making the predictions by utilizing a database having a number of observations and generating reduced-order models that can be used in the preliminary design exercises. In present work, we created a CFD database having 100 observation points with three varying design variables: strut location, strut wedge angle and strut V-settlement angle. We applied Artificial neural network regression model to this database in order to formulate the mixing efficiency of multi-strut injection scramjet engine. We discuss the deep learning model prediction accuracy by computing coefficient of determination, R^2 and drawing the parity plots for each objective function. In our findings in the investigation of the flow physics, the wedge angle is the dictating parameter for the shock-expansion wave structure in the post strut region and accordingly the mixing and aerodynamic performance of the engine.

Keywords: *high-speed propulsion, hydrogen fueled engine, multi-strut injection, machine learning, mixing efficiency, total pressure recovery factor*

1. Introduction

Dual mode ramjet (DMR) engines are considered as the power unit of hypersonic air transportation systems in near future. It has many advantages such as no need for carrying on-board oxidizer or any rotating component in the propulsive path, however, the flow along the duct is quite complex and needs

[1] *PhD Candidate, VKI (von Karman Institute for Fluid Dynamics), Aeronautics and Aerospace Department, Chaussée de Waterloo 72, Rhode-Saint-Genese, ali.can.ispir@vki.ac.be*

[2] *PhD Candidate, Université Libre de Bruxelles, École polytechnique de Bruxelles, Aero-Thermo-Mechanics Laboratory, kamila.zdybal@ulb.be*

[3] *Research Expert, VKI (von Karman Institute for Fluid Dynamics), Turbomachinery and Propulsion Department, Chaussée de Waterloo 72, Rhode-Saint-Genese, saracog@vki.ac.be*

[4] *Assistant Professor, VKI (von Karman Institute for Fluid Dynamics), Aeronautics and Aerospace Department, Chaussée de Waterloo 72, Rhode-Saint-Genese, magin@vki.ac.be*

[5] *Professor, Université Libre de Bruxelles, École polytechnique de Bruxelles, Aero-Thermo-Mechanics Laboratory, axel.coussement@ulb.be*

to be modelled carefully in the consideration of the challenges in modeling of fuel-air mixing, ignition, thermal choking phenomena and so on [1]. The designing the mixing process has huge importance in terms of not only non-premixed combustion efficiency in the scramjet, but also, overall system performance influencing net thrust and aerodynamic internal losses [2]. Researchers and scramjet designers have focused on inventing a way to provide optimal fuel-air mixing distribution and augment the mixing efficiency without sacrifing aerodynamic effectiveness [3, 4]. Among those methods, injecting the fuel into the high-speed air stream in parallel and generating a penetration zone throughout shock-expansion waves structure behind fuel struts can promise an effective solution [5]. The strut design parameters become significant in this sense since they orient the wave structure in the reactive zone and form the mixing and accordingly the burning processes. In this regards, there are many efforts in literature which were devoted to investigate the design parameters of the injection. Sujith et al. performed experimental and numerical studies to examine the effect of trailing ramp angle on supersonic mixing efficiency with various angles and two configurations [6]. In their findings, the highest total pressure loss was seen in the sample demonstrated best mixing performance. It was noted that vorticity generated by the struts influenced the mixing positively nevertheless caused a remarkable loss in the total pressure term. Manna et al. investigated different fuel injection strut arrangements with various combustor inlet flow conditions in order to observe their effects on combustion efficiency, engine thrust, heat release and total pressure loss [7]. The authors concluded that incurred drag losses due to the injectors significantly affect the thrust more than combustion and mixing efficiencies. Choubey and Pandey run numerical simulations on the scramjet test facility of DLR to compare two different strut configurations with the different angles of attack (AoA) of fuel injectors in terms of aforementioned performance parameters [8]. They found that multi strut configurations had a beneficial impact on performance parameters while the maximum combustion efficiency and smallest ignition time were provided when injector's AoA was set as zero. On the other hand, flight conditions i.e. flow variables of the incoming air have important effects on the engine performance as well as the strut geometries and configurations. Reddy and Venkatasubbaiah performed numerical studies on the same case with Choubey and Pandey, and found also that multi strut injector arrangement provides better performance than single strut [9]. They also conducted conducted the numerical analysis with different flight conditions and noted that increasing of total pressure and temperature with the flight speed led the combustion efficiency to rise. Huang and Yan investigated ram - scram transition mechanism in a strut-based dual-mode scramjet combustor by performing numerical simulations at cruise speeds between Mach 4 and 7 [10]. They showed that inlet boundary conditions higher freestream Mach number is more favorable for the fuel - air mixing process. However, they also noted that the mixing efficiency did not vary after the freestream Mach number exceeds a certain threshold.

Reduced-order models (ROM) i.e., the models based on zero-and-one dimensional approaches are commonly preferred to asses the performance of the dual-mode ramjet engines [11, 12, 13]. They are considered as cost-effective solutions for instance in performance estimation and feasibility analysis, and also inseparable parts of the conceptual design works. To improve the accuracy of the performance assessment studies of the high-speed air-breathing engines, surrogate assisted evolutionary algorithms and reduced order modelling techniques are widely utilized in reactive and non-reactive flow applications [14, 15, 16, 17]. We consider that these approaches and coupling with fuel-air mixing supersonic numerical dataset could enable us to explore the entire design space of the scramjet engine and create machine learning models which are functions of strut geometric design parameters and represent well the fuel-air mixing phenomena.

In the present article, we solved 2D RANS filtered compressible flow equations on a dual-mode ramjet engine combustor domain to investigate the fuel-air mixing phenomena comprehensively as a function of strut configurations. We computed the mixing efficiency at several stations and total pressure recovery factor to discuss the struts' geometrical impacts on the mixing and aerodynamic features of the combustor component. We generated a CFD database including the the mixing efficiencies and total pressure recovery factor at 100 observation points and it enabled us to conduct a thoroughgoing discussion on the fuel-air mixing phenomena in the multi-strut injection scramjet engine. We also coupled the dataset with Artificial neural network to create a machine learning model for making the prediction in unexplored

points by the CFD. The model is basically a sort of reduced-order model representing the fuel-air mixing features in the multi-strut scramjet engine as a function of strut configuration parameters.

2. Methodology

2.1. Engine specifications and numerical model:

The numerical investigations were done on a 8.4 meter length DMR combustor in which the fuel is injected into the high-speed air stream via 23 fuel struts and 1248 injectors. The fuel struts are V-shaped and have an angle of 52.3^0 with the center axis, the top and bottom wedge angles of them are 168^0. The incoming air flow and engine geometry data were provided by Italian Aerospace Research Center (CIRA) [18]. The air flow enters the combustor with 33.7kPa static pressure, 871K static temperature and speed of Mach 3.4 in average. These inflow conditions are representative of the DMR engine operating at 33km altitude with the cruise speed of Mach 8. The total pressure and temperature of fuel at the injectors is given as 73.4bar and 610K, respectively, and the equivalence ratio is defined as 0.65.

The 2D compressible and non-reactive Reynolds averaged Navier-Stokes equations (Eqs. 1 - 3) coupled with species transport (eq. 4) and k - ω SST turbulence equations, were solved by Ansys Fluent, commercial CFD code for the flow in the multi-strut injection DMR engine combustor under investigation. in the governing equations set, ρ is the density, $\vec{v}$ is the velocity, E is the total energy, P is the pressure, k_{eff} is the effective thermal conductivity, h_i is the enthalpy of species i, $\overline{\overline{\tau}}$ is the viscous stress tensor, Y_i is the mass fraction of species i. Since the oxidation of hydrogen with air is out of scope of this work, reactive and source terms are not involved into the governing equations. k - ω turbulence model was noted as very effective predictor to resolve the interaction between shock - expansion waves and mixing layer [14, 19]. Compressible real gas Navier-Stokes/Euler equation set which is highly recommended for density variations, multi-species flows and flows in which the global Mach number is generally higher than about 0.2 [20]. The mass diffusive flux ($\vec{J_i}$) for i^{th} specie (H_2, N_2 and O_2) is solved by eq. (5) with Schmidt number (Sc_t), mass ($D_{i,m}$) and thermal ($D_{T,i}$) diffusivities. In the present work, we assume Lewis number $Le = 1$ and Schmidt number $Sc = 0.7$. The thermal diffusivity was computed by Soret equation [21]. The boundary conditions of the simulations of the multi-strut injection scramjet engine are shown in Fig. 1 and Table 1. The inlet boundary conditions were defined as nonuniform and the values were interpolated from the 3D CFD simulations [18].

$$\nabla \cdot (\rho \vec{v}) = 0 \tag{1}$$

$$\nabla \cdot (\rho \vec{v} \vec{v}) = -\nabla P + \nabla \cdot \overline{\overline{\tau}} \tag{2}$$

$$\nabla \cdot (\vec{v}(\rho E + P)) = \nabla \cdot \left(k_{eff} \nabla T - \sum_i h_i \vec{J_i}\right) + \nabla \cdot (\overline{\overline{\tau}} \cdot \vec{v}) \tag{3}$$

$$\nabla \cdot (\rho Y_i \vec{v}) = -\nabla \cdot \vec{J_i} \tag{4}$$

$$\vec{J_i} = \left(\rho D_{i,m} + \frac{\nu_t}{Sc_t}\right) \nabla Y_i - D_{T,i} \frac{\nabla T}{T} \tag{5}$$

2.2. Design variables and objective functions:

Fuel-air mixing phenomena in a multi-strut injection DMR engine was explored with three design variables; struts location, ϕ_1, and struts settlement angle, ϕ_2, and strut wedge angle, ϕ_3, as drawn in the top view of the combustor scheme (fig. 2a). The fuel-air mixing process is strongly influenced by the shock-expansion waves structure as mentioned above. The fuel stream injected by one strut into high-speed air flow is oriented by the wave structure created by the entire struts set. Hence, the idea behind the selection of these strut parameters is to observe how each strut configuration parameter causes significant alteration on the formation of the wave structure and accordingly how it affects the mixing process

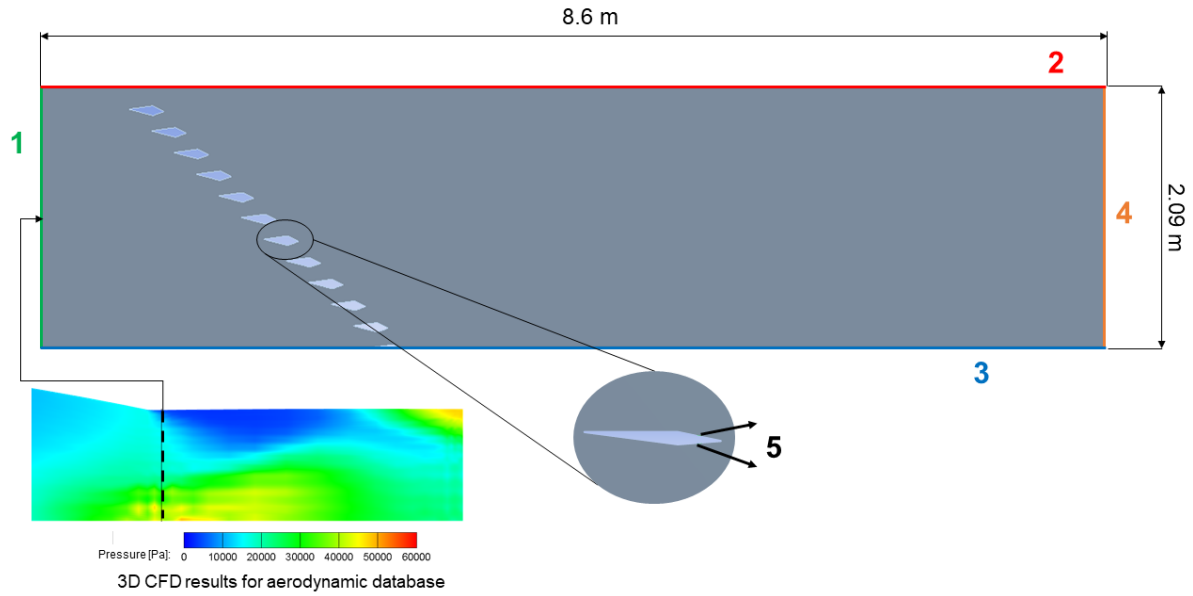

Fig 1. The boundary conditions of the scramjet engine studied in the present paper.

Table 1. The boundary conditions defined for the simulations of multi-strut injection scramjet engine as shown in Fig. 1.

Station	Zone name	Boundary condition	Details
1	Air-inlet	Pressure far field	Mach $= 3.4$, $T = 871K$, $P = 31kPa$ (average)
2	Wall	Adiabatic wall	-
3	Center-axis/symmetrical plane	Symmetrical	-
4	Outlet	Pressure outlet	-
5	Fuel inlet	Mass flow inlet	ER $= 0.65$, $T_0 = 612K$, $P = 2.02bar$ for upside, and $P = 2.14bar$ for downside injectors

and aerodynamic features in terms of the losses on the total pressure recovery factor. Examination of these parameters is also important to determine the engine design limits and performance linking to supersonic fuel-air mixing and combustion physics. The range of these design variables are given as [0 - 10] x 600mm, 32.3^o - 62.3^o and 138^o - 168^o for strut location, V-settlement angle and wedge angle, respectively.

The strut configuration on the fuel-air mixing process is evaluated throughout two critical parameters which are mixing efficiency which computed at 20 stations having 10cm interval between them along the x-axis on the duct and total pressure recovery factor as given eqs. 6 - 8 and shown in fig. 2b:

$$\eta_{mix}(x) = \frac{\dot{m}_{fuel,mixed}}{\dot{m}_{fuel,total}} = \frac{\int Y_{react}\rho U dA}{\int Y \rho U dA} \tag{6}$$

$$Y_{react} = \begin{cases} Y, Y \leq Y_{stoich} \\ \frac{(1-Y)Y_{stoich}}{1-Y_{stoich}}, Y > Y_{stoich} \end{cases} \tag{7}$$

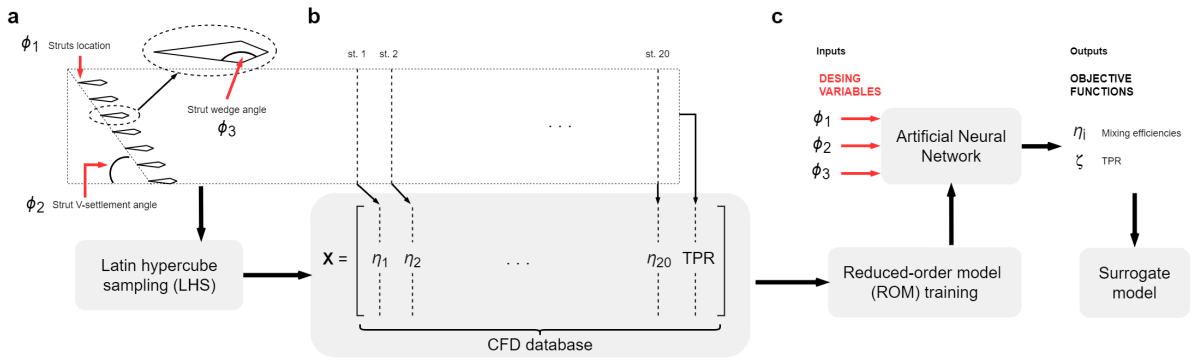

Fig 2. The design variables selected for CFD database generation

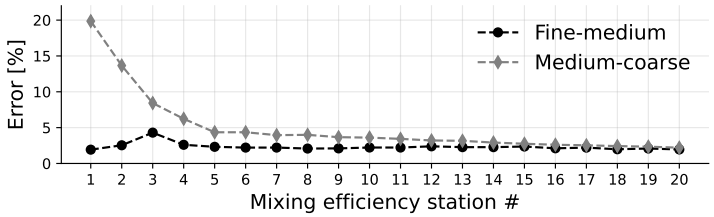

Fig 3. The error percentage between the investigated grids for the mixing efficiencies computed at 20 stations.

$$\zeta = \frac{p_{t,outlet}}{P_{t,inlet} + P_{t,fuelinjectors}} \tag{8}$$

2.3. Mesh independency:

We performed grid independence work for the numerical simulations of the multi-strut DMR combustor in order to detect optimal number of elements by following a guideline proposed by Celik et al. [22]. For this purpose, the 2D DMR combustor domain was meshed with unstructured and structured quadrilateral grid types and three different number of elements, coarse (1.47M elements), medium (2.3M elements) and fine (4.7M elements). The analysis were performed with a workstation having 128-core AMD 1.8GHz with 1TB RAM. To achieve Y+ value as less than 1 in the entire flow domain, the mesh near the struts' walls was fined and 0.001mm mesh size was used for the first height. The optimum number of elements was determined by computing and comparing the error rates of mixing efficiencies in 20 stations and total pressure recovery factor which were detailed in the sec. 2.2. The error rate (as per [22]) between the mixing efficiencies (computed with three different number of elements) and TPR are shown in fig. 3 and also in Table 2.

Table 2. Refinement ratio, error rate in total pressure recovery factor (ζ) and computational time for three analyzed grids with different number of elements.

# of elements	$(N_{coarsen}/N_{refine})^{0.5}$	Error [%] in ζ (coarsen - refine)	Computational time [h])
4.7M	1.32	1.53	278.84
2.3M	1.61	1.27	166.49
1.47M	-	-	81.17

2.4. Regression of the CFD database:

A CFD database including 100 observations was created by using the numerical modeling given above and the data points were determined by Latin hypercube sampling (LHS) method [23]. The fig. 2c

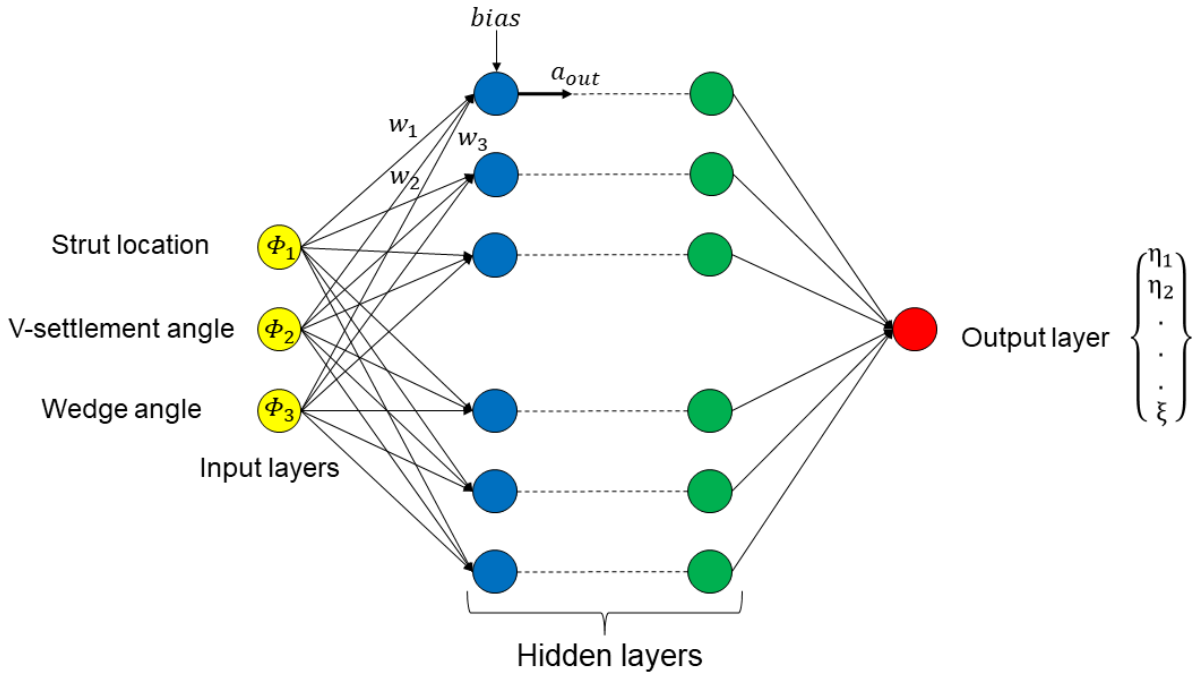

Fig 4. Schematic illustration of a deep neural network model built for the present problem.

summarizes the process to generate surrogate model for fuel-air mixing process. The present work aims to obtain a ROM for the mixing efficiency as a function of the duct x-axis and investigated strut geometrical parameters as depicted in eq. 9. We thus regressed mixing efficiencies at 20 stations and TPR.

$$\eta_i(x) = f(\phi_1, \phi_2, \phi_3) \tag{9}$$

The ANNs which are inspired by the biological neural structures consisting of interconnected network of neurons. An ANN model architecture is composed of input layer, a number of hidden layers and output layer as depicted in Fig. 4. The ANN models for regression of the objective functions were constructed on the Keras platform [24]. The model basically aims to build a representative mathematical pattern between inputs and outputs of a given dataset to make prediction on the points that are not explored [25]. The information provided by the inputs are transferred via neurons in the consecutive layers with weights, w, biases, b, and activation functions, f. The weights quantify the impact of each input on the output while the biases are used as adjustment constants for each layer. The calculation of an output from a neuron in the j^{th} layer, is shown in eq. 10.

$$a_{out} = f_j\left(b_j + \sum_i^N a_i w_i\right). \tag{10}$$

For the regressions of all of the objective functions, rectified linear activation function (ReLU) performed better than other activation functions (such as sigmoid or hyperbolic tangent). Thus, we selected ReLU to activate hidden layers and activated output layer with a linear function to allow for unbounded output values. The prediction performance of the built ANN model highly depends on the selection of the hyper-parameters which compose of hidden layers, number of neurons in each hidden layer, or learning rate. Random search method [26] which is available in the Keras platform, is used to find the optimal hyper-parameters for each ANN structure built in the current work. It is worth to mention also that the ANN

prediction performance strongly depends on how the inputs to the network are scaled. To determine the best scaling for the input parameters, we utilized a proposed cost function, $\mathcal{L}$, that can facilitate to assess the quaility of the data parameterization for the regression [27, 28]. Minimizing the cost value allows us to determine which scaling factor should be applied on the design variables (independent variables) to yield promising regressibility of each objective function (dependent variables). The individual costs $\mathcal{L}_i([\widetilde{\phi}_1, \widetilde{\phi}_2, \widetilde{\phi}_3], \eta_i)$ for mixing efficiency parameters and $\mathcal{L}_i([\widetilde{\phi}_1, \widetilde{\phi}_2, \widetilde{\phi}_3], \zeta)$ for the total pressure recovery factor were computed, where tilde denotes a scaled value. The best choice of scaling which led to the minimum cost value, $\mathcal{L}_i$, were noted in Table **??**. Particularly, each independent variable in the input matrix, ϕ_i, is divided by its standard deviation, s, in Auto scaling, by $\sqrt{s}$ in Pareto scaling, by $s^2/\text{mean}(\phi_i)$ in VAST scaling. The $\langle -1, 1 \rangle$ scaling scales each variable to the $\langle -1, 1 \rangle$ range.

The ANN prediction performance is assessed by checking the coefficient of determination, R^2. The closer R^2 is to unity, the better the regression model predictions. The data matrix is divided into a number of bins (5-10) in the assessment because the overall R^2 computed for all points in the dataset can be misleading. The R^2 is computed in each bin to investigate the prediction performance thoroughly [28]. This approach enables us to have an ANN model which represents the entire dataset rather than focuses on any specific region. In the j^{th} bin we thus computed the metric with eq. 11.

$$R_j^2 = 1 - \frac{\sum_{i=1}^{N_j} (\phi_{o,i}^j - \phi_{p,i}^j)^2}{\sum_{i=1}^{N_j} (\phi_{o,i}^j - \text{mean}(\phi_o^j))^2}, \tag{11}$$

where N_j represents the number of observations in the j^{th} bin. For the i^{th} dependent variable in the j^{th} bin, $\phi_{o,i}^j$ and $\phi_{p,i}^j$ represent observed and predicted outputs, respectively. While global errors are shown in Table **??**, the local errors are depicted by the parity plots (Fig. 6) given in Sec. 3.2.

3. Results

3.1. Regression assessment and machine learning model of fuel-air mixing:

In this section, we assess and discuss the Artificial neural network regression model performance in the context of predicting mixing efficiency and ζ. Numerical simulations for investigating the fuel-air mixing phenomena are included in the CFD database corresponding to various design variables. The obtained data matrix, **X**, colored by the objective functions is demonstrated in Fig. 5. It can be clearly seen that there is a trade-off between mixing efficiency and ζ. The general trend of the graphs indicates that the wedge angle has a greater impact on each objective function. The interaction between the fuel-air streams increases with the closeness of the struts when the V-settlement angle parameter is set to higher values. The closer fuel struts to each other, the wave structures created by each of them affect the others' stream formation more. Even though the better mixing efficiency is obtained with the smaller wedge angle, as seen in the map of η_1, the bigger wedge angle gives better result with the low V-settlement angle. One of the root causes for this observation, is that the hydrogen could spread with by creating the wide vortexes as attributed to the lower wedge angle and create pure fuel zones behind the struts instead of penetrating into the air-stream. A greater V-settlement angle could compensate the situation by increasing the interaction between the flow streams and allow more air flow to be mixed with the fuel. However, the better η_1 can be also provided with the bigger wedge angle in the region where less interactions is observed due to the lower V-settlement angle. Because the low V-settlement angle allows more air flow to interact with the fuel stream. While this has a slight impact on the mixing efficiency values in the region close to the fuel struts, this observation diminishes in the mixing efficiencies computed in the further stations. Since the strut location is related with the initial interaction between the fuel streams and shock wave of the incoming high-speed air, the effect of it on the objective functions varies with the selection of the other design variables. This makes it difficult to understand the trend between the injection position and the objective functions and accordingly to construct mathematical pattern between independent design variables and outputs. The present paper is thus dedicated to discovering the non-linearity of the current problem using deep learning methods.

Table 3 collects results for the hyper-parameter tuning in the Artificial neural network models built for the mixing efficiency η_i and ζ. The hyper-parameters of the twenty-one network models were optimized by

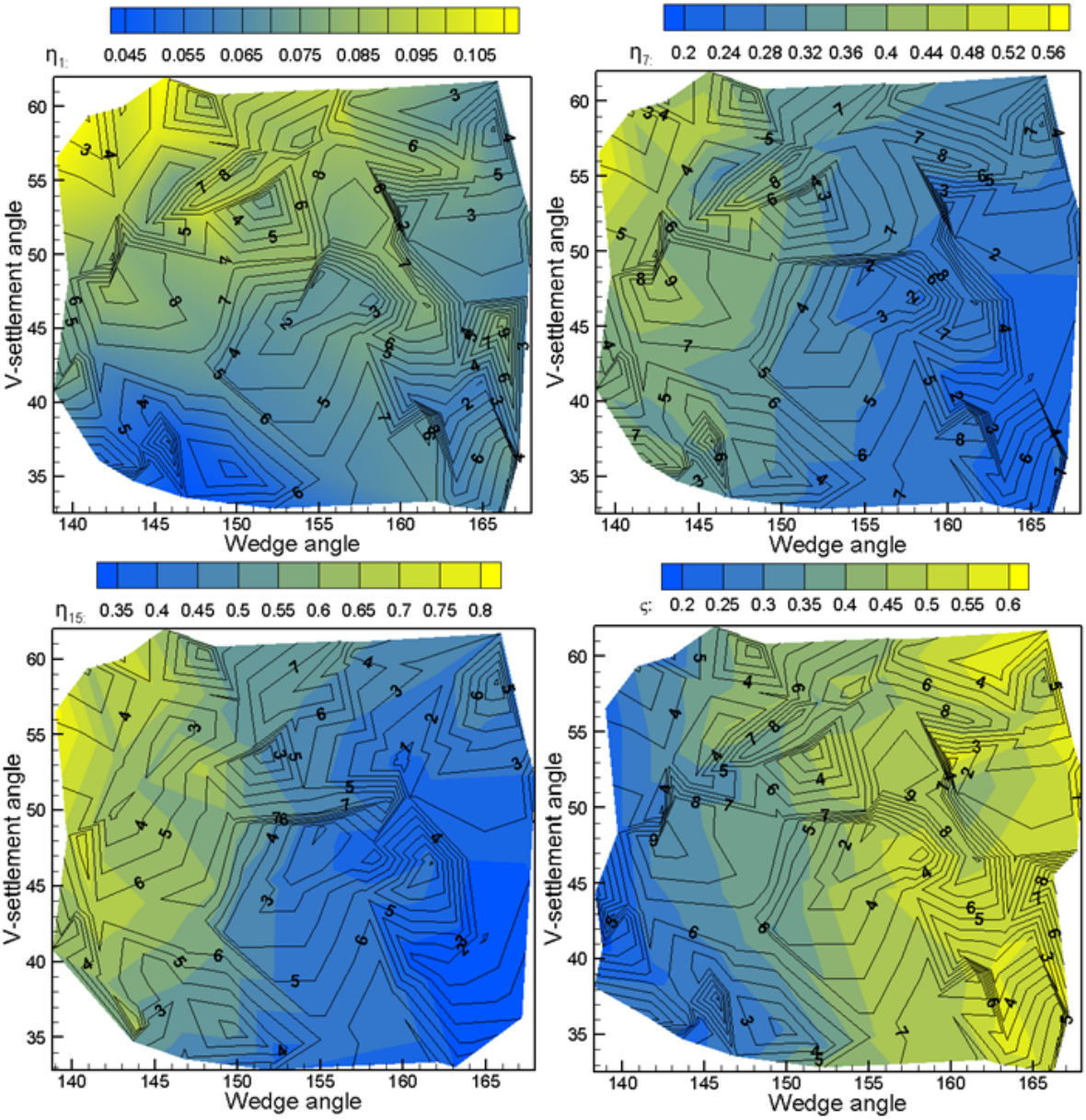

Fig 5. Mixing efficiencies, η_1, η_7, η_{15}, and TPR values, ζ, in the space of the V-settlement angle and the wedge angle. Solid intersecting lines represent the strut location design variable.

following the methodology given in sec. 2.4. In all regressions, 80% of the whole dataset was selected to train the data and the rest was used to validate the model. As pointed before, R^2 value computed for the whole trained dataset can be misleading, hence we first examined the values in each bin as per sec. 2.4. While the overall metrics are shown in Table 3, the parity plots of some of the regressed parameters given in fig 6 enable one to see the error rates between the predicted and the observed points. Since the data is very chaotic in the region close to the injection points, the ANN models struggled to train the entire dataset as understood from the parity plots and also, overall R^2 values. Although the error rate computed between predicted and observed points is over than 20 % in some observations, it does not have significant detrimental impact on the mixing efficiency profile. Therefore, we can say that the machine learning model composed of the activation function, weight and biases and built for each mixing efficiency station, represents the fuel-air mixing formulation as a function of investigated strut design parameters.

Table 3. The optimized hyper-parameters of the Artificial neural network that yield the best R^2 value. The hyper-parameters are respectively: scaling factor, the number of hidden layers, cost for independent parameter optimization, $\mathcal{L}_i$, and the learning rate, α. We also show the overall R^2 values obtained for each objective function.

Obj. Fun.	Scaling	# Hid. lay.	$\mathcal{L}_i$	α	R^2
η_1	VAST	7	1.05	0.0001	.96
η_2	Auto	14	1.22	0.0001	.98
η_3	Auto	17	1.19	0.0001	.98
η_4	Auto	8	1.22	0.0001	.99
η_5	Auto	15	1.27	0.0001	.97
η_6	Pareto	18	1.16	0.0001	.98
η_7	Pareto	7	1.11	0.0001	.99
η_8	Pareto	11	1.08	0.0001	.99
η_9	Pareto	10	1.07	0.0001	.98
η_{10}	Pareto	15	1.07	0.0001	.98
η_{11}	Pareto	18	1.06	0.0001	.99
η_{12}	Auto	15	1.09	0.0001	.99
η_{13}	Auto	21	1.09	0.0001	.99
η_{14}	Auto	10	1.09	0.0001	.99
η_{15}	Auto	10	1.09	0.0001	.99
η_{16}	Pareto	19	1.07	0.0001	.99
η_{17}	Auto	12	1.11	0.0001	.98
η_{18}	$\langle -1, 1 \rangle$	12	1.15	0.001	.99
η_{19}	$\langle -1, 1 \rangle$	14	1.14	0.001	.99
η_{20}	Pareto	12	1.08	0.0001	.99
ζ	VAST	15	1.06	0.0001	.98

3.2. Impact of the design variables on the fuel-air mixing process:

The multi-struts set geometric parameters impact on the mixing and aerodynamic performance of the combustor are investigated with respect to fuel penetration into the high-speed air stream, mixing efficiency, and losses on the total pressure recovery factor. Some of observations were used to carry out the discussion in this section. Their strut design parameters and mixing efficiency profiles were demostrated in Table. 4 and fig. 7. It was observed that the wedge angle has an importance on the objective functions since it can be considered as the dictating parameter of the formation of the shock-expansion wave structure in the post-injection zone. Due to the presence of the non-uniform flow distribution along the

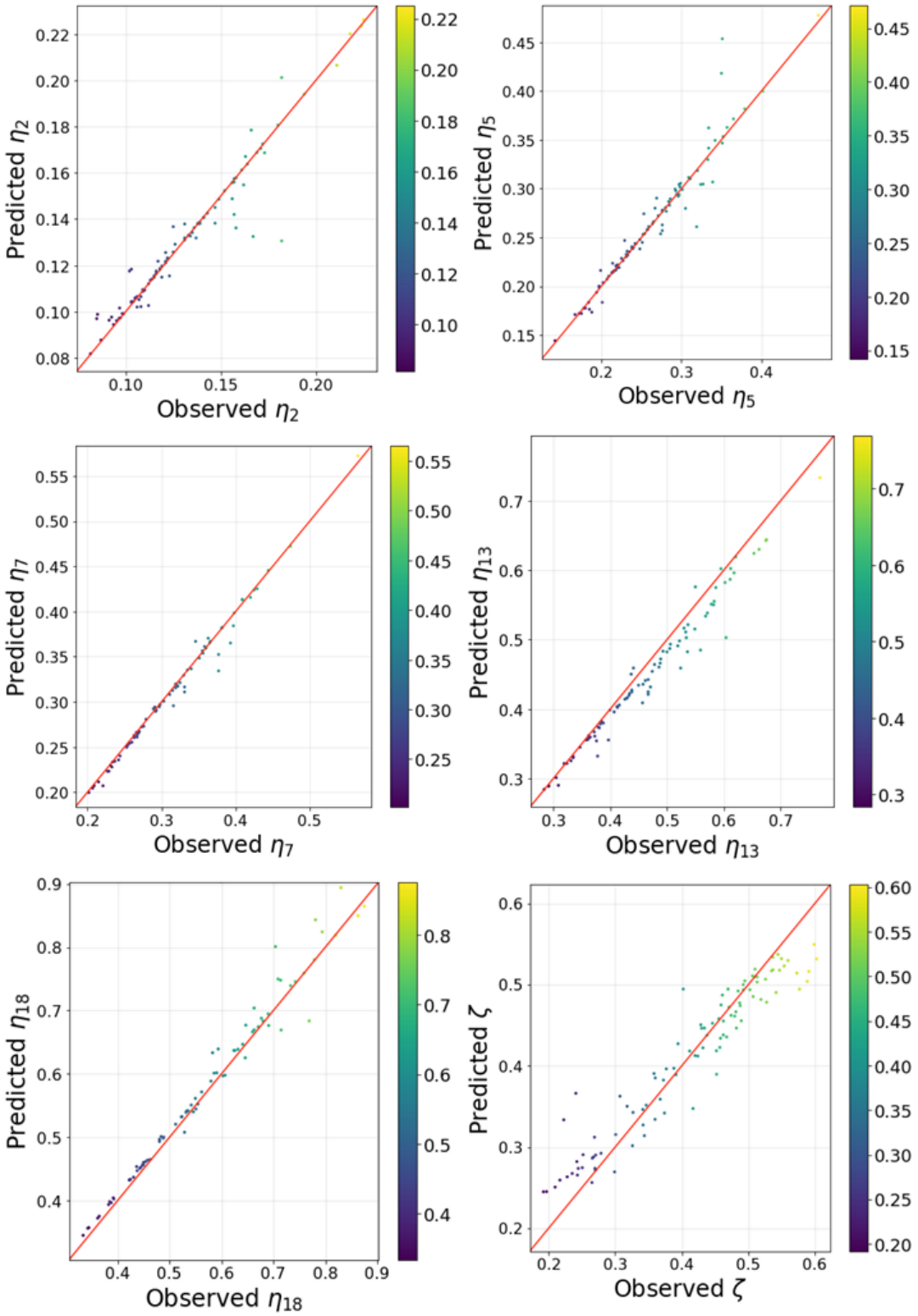

Fig 6. Parity plots of some of the selected objective functions predicted by the Artificial neural network.

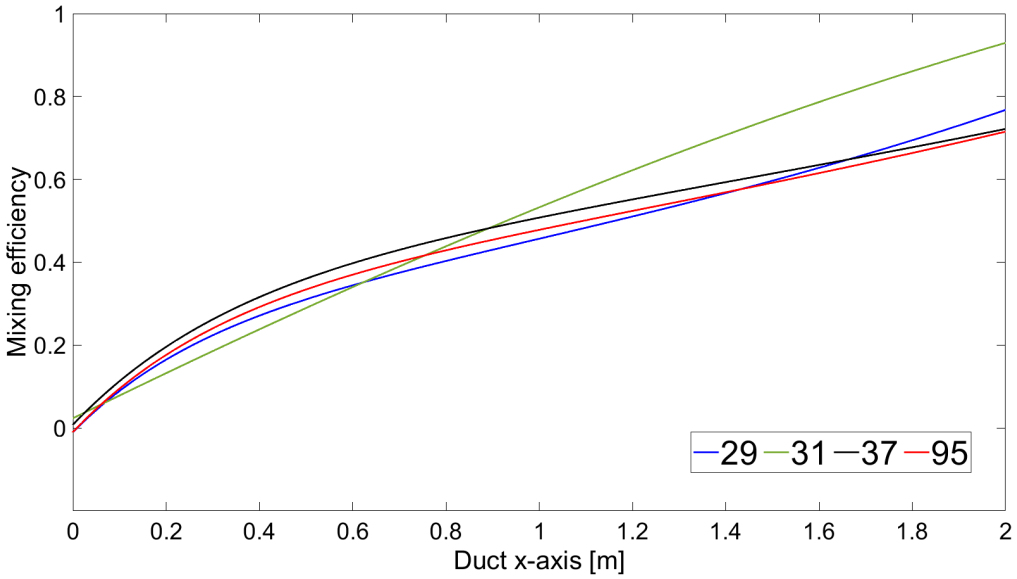

Fig 7. Mixing efficiency profiles for a selected number of observations from the CFD dataset.

combustor inlet, attack of angle (AoA) of the incoming high-speed air stream varies along the both axis. Even a small change on AoA could make an important impact on the mixing process by causing the normal shock or oblique shock wave generation in the leading edge of the struts. This is strongly linked to the flow separation and shock-shear layer interaction and highlights the significance of the selection of the V-settlement angle and strut location design parameters. The change of AoA makes the difference on the orientation of secondary and tertiary compression zones as seen in fig. 8 for three random observations. It can be clearly seen that the sizes of recirculation zones differed with the presence of the normal and oblique shocks. Especially, the comparison of the observations of 29 and 31 which have similar wedge and V-settlement angles, emphasises the significance of the strut location. Setting the strut location to the further for the observation 31 caused the normal shock to generate in the leading edge and the air flow to decelerate into subsonic conditions. The presence of the normal shock seen in the observation of 31 affected also the fuel stream orientation and led to enlarging of the surface area of the counter-rotating vortexes. This made a positive influence on the mixing level while the normal shock made an adverse effect on the TPR.

Table 4. TPRs (ζ) for the observations selected for the discussion.

Observation number	ϕ_3	ϕ_2	ϕ_1	ζ
29	138.8	40.8	2.0	0.19
31	139.3	42.7	6.4	0.22
37	145.6	62.0	4.4	0.39
95	148.7	60.8	3.3	0.42

It is also worth to emphasize the importance the incoming shock wave caused by the nonuniform combustor inlet for its interaction with the mixing zone and alteration of the wave structure in the mixing region. It affects the mixing process with either intersecting one fuel stream or blocking the stream propagation after it is reflected by the adiabatic wall. The reflected shock wave interacted with the shock pattern in the post-strut zone and boosted regional pressure level. By this way, the flexibility of fuel stream along the x-direction diminishes and it is pressed and forced slightly to spread along the y-direction. This increases the mixing efficiency and reduces the mixing length. It was found that the greatness of

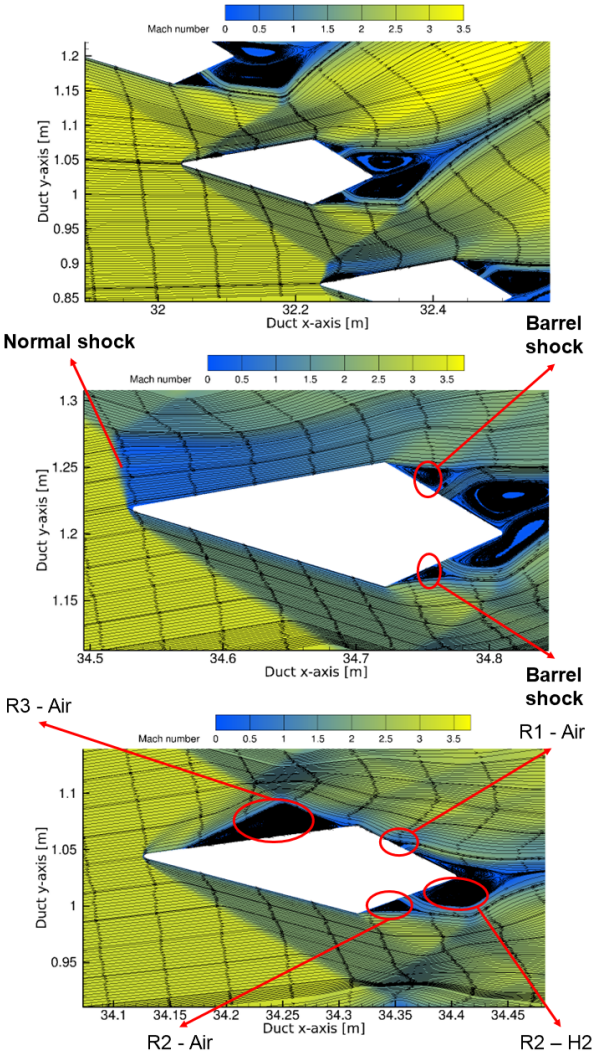

Fig 8. The mach number contours of Cases of 29, 31 and 37 (from top to down) with re-circulation zones.

the reflected shock wave highly depends on the wedge angle. Moreover, V-settlement angle and strut location were found important in terms of where and how the wave interacts with the struts and mixing zone. In the comparison of the observations numbered with 31 and 37 as seen in fig. 8 and 9, the struts set is chosen closer to the inlet in the sample 37 and more struts and fuel streams encountered with the pressure wave coming from the intake and this amplified the oblique shock intensity especially near the symmetry axis. Due to this reason, the observation 37 showed better mixing performance until 0.5m distance from the injection points as drawn in fig. 7. However, in further region, the importance of having lower wedge angle came into prominence and made the flow in the observation 31 encounter stronger oblique shock wave as indicated in fig. 9. The dominance of the wedge angle can be also easily distinguished in the comparison of the observations of 37 and 95 by looking on the pressure distribution with fuel stream propagation and and mixing efficiency profiles (Fig. 7). Even though both observations have similar V-settlement angle and strut location, even 3-degree wedge angle difference causes big gap in the mixing efficiency profiles in the far field region.

Thanks to the investigation of the strut location design variable, it was possible to comprehend the effects of the distance between the injection point and throat of the combustor on the mixing and aerodynamic features of the engine. The proper mixing of two different streams needs space/time. In some observations, the fuel flow left the combustor without being mixed with the air and it is very sure that the unburnt rate of the hydrogen will be remarkably high and engine performance will be affected adversely. On the other hand, placing the struts close to the exit of the duct made a slight positive impact on the ζ since the shock-expansion wave structure are not constructed, yet. However, in some observations having moderate strut location i.e. which the fuel is injected into the air around mid of the combustor, the selection of the lower wedge angle provides rapid mixing and mixing efficiency and reduces the pure hydrogen rate at the outlet consequently. As considering the adverse effects on the aerodynamic performance, the wedge angle and strut location must be optimized to find the best solution for the mixing and aerodynamic efficiencies in this sense.

4. Conclusion and Discussion

In the present work, we investigated supersonic fuel-air mixing phenomena in a multi-strut scramjet engine combustor and built an Artificial neural network structure to create a model which can represent the mixing and explore the design space of the strut configuration. We also computed total pressure recovery factor in order to discuss the trade-off between the mixing and aerodynamic performance of the combustor. For these, we solved the RANS filered compressible flow equations and generated a CFD database including 100 data observations, each with varying strut configuration parameters: strut wedge angle, strut V-settlement angle and strut location. The data points were determined by the Latin hypercube sampling design of experiment method. In below, we present our findings and conclusions from the current study:

- The mixing efficiency was integrated along the 20 stations on the duct axis and total pressure recovery factor was computed between inlet and outlet of the combustor. The ANN model was constructed for each objective function (21) and prediction accuracy was measured by computing R^2 coefficient of determination value. Since the mixing efficiency data close to the struts are bit more chaotic, the overall R^2 values here are relatively low as compared to the ones in other zones. The parity plots enabled us to view the local errors. Even though the error rate in some points are high, this error does not make any important adverse impact in the general profile of the mixing efficiency.

- In the present problem, the fuel-air mixing took place throughout shock-expansion waves structure generated by the fuel struts. The process is substantially influenced by the greatness and orientation of this structure which are determined by the investigated strut design parameters. We found the strut wedge angle is the dominant parameter for the formation of the shock-expansion wave in behind the struts.

- It was observed that an incoming shock wave defined by the nonuniform boundary condition of the air inlet could significantly affect the mixing process. The angle, direction, and greatness

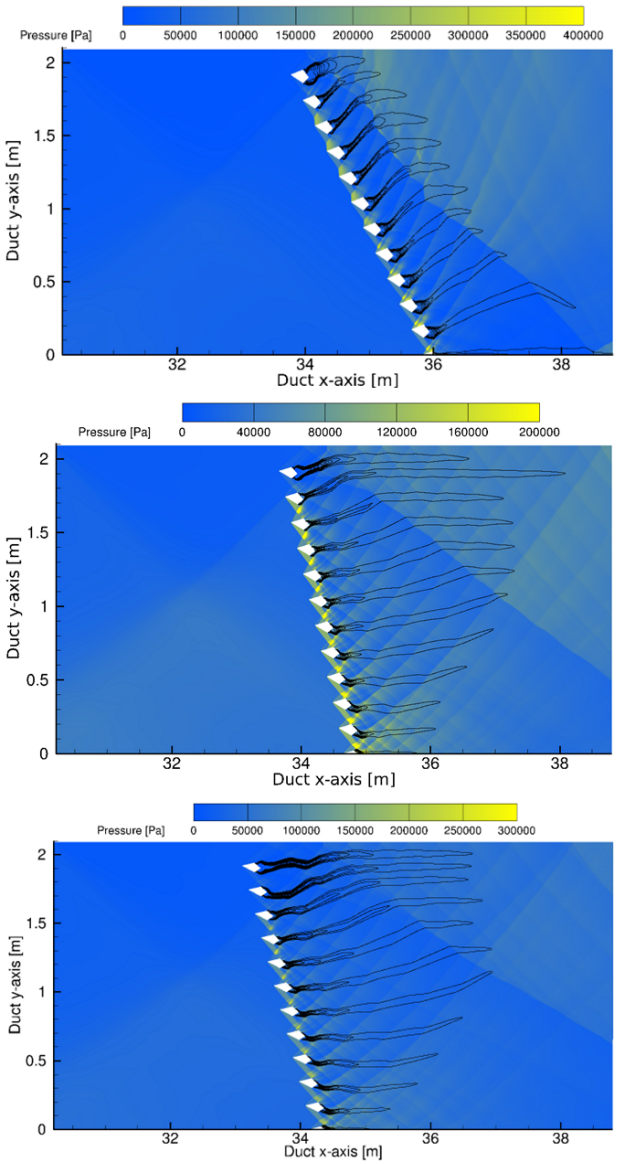

Fig 9. The pressure contours of observations 31, 37 and 95 (from top to down) with fuel streamlines.

of the incoming wave have importance when it interacts with the fuel streams. This thus emphasizes the significance of selection of the V-settlement angle and strut location parameters. They play also very essential roles on the generation of the secondary and tertiary compression zones, counter-rotating vortex pairs which directly affect the orientation and penetration of the fuel stream. The wrong combination could also led to the occurrence of the normal shock wave at the leading of the struts which brought about adverse effects on the total pressure recovery factor.

- We also observed that an enough distance is needed to obtain a proper fuel-air mixing. Approaching the fuel injectors by setting the strut location to its corresponding values, too close to the combustor exit can make slight positive impacts on the total pressure recovery factor since the shock-expansion wave structure does not have time/space to form. However, the mixing efficiency was computed quite low in the observations having big strut locations. Even though the low wedge angle in such cases could compensate the lowness of the mixing effectiveness by causing the generation of strong turbulent flow behind the struts, the distance may not enough for a chemical reaction of the hydrogen-air mixture. Thus, the design variables are highly recommended to be optimized by considering also the combustion.

Acknowledgments

This project has received funding from the European Union's Horizon 2020 research and innovation programme under grant agreement No 101006856.

References

[1] H. Ogawa. "Mixing characteristics of inclined fuel injection via various geometries for upstream-fuel-injected scramjets". In: *Journal of Propulsion and Power* 31.6 (2015), pp. 1551–1566. DOI: 10.2514/1.B35581.

[2] Ji-Ho Kim et al. "Numerical study of mixing enhancement by shock waves in model scramjet engine". In: *AIAA journal* 41.6 (2003), pp. 1074–1080. DOI: 10.2514/2.2047.

[3] KM Pandey and T Sivasakthivel. "Recent advances in scramjet fuel injection-a review". In: *International Journal of Chemical Engineering and Applications* 1.4 (2010), p. 294. DOI: 10.7763/IJCEA.2010.V1.52.

[4] Z Gao and C Lee. "Numerical research on mixing characteristics of different injection schemes for supersonic transverse jet". In: *Science China Technological Sciences* 54.4 (2011), pp. 883–893. DOI: 10.1007/s11431-010-4277-9.

[5] Juntao Chang et al. "Research progress on strut-equipped supersonic combustors for scramjet application". In: *Progress in Aerospace Sciences* 103 (2018), pp. 1–30. DOI: 10.1016/j.paerosci.2018.10.002.

[6] S Sujith, TM Muruganandam, and Job Kurian. "Effect of trailing ramp angles in strut-based injection in supersonic flow". In: *Journal of Propulsion and Power* 29.1 (2013), pp. 66–78. DOI: 10.2514/1.B34532.

[7] P Manna, Ramesh Behera, and Debasis Chakraborty. "Liquid-fueled strut-based scramjet combustor design: a computational fluid dynamics approach". In: *Journal of Propulsion and Power* 24.2 (2008), pp. 274–281. DOI: 10.2514/1.28333.

[8] G Choubey and KM Pandey. "Effect of variation of angle of attack on the performance of two-strut scramjet combustor". In: *International Journal of Hydrogen Energy* 41.26 (2016), pp. 11455–11470. DOI: 10.1016/j.ijhydene.2016.04.048.

[9] P Nithish Reddy and K Venkatasubbaiah. "Numerical investigations on development of scramjet combustor". In: *Journal of Aerospace Engineering* 28.5 (2015), p. 04014120. DOI: 10.1061/(ASCE)AS.1943-5525.0000456.

[10] Wei Huang and Li Yan. "Numerical investigation on the ram–scram transition mechanism in a strut-based dual-mode scramjet combustor". In: *International Journal of Hydrogen Energy* 41.8 (2016), pp. 4799–4807. DOI: 10.1016/j.ijhydene.2016.01.062.

[11] Duo Zhang et al. "Quasi-one-dimensional model of scramjet combustor coupled with regenerative cooling". In: *Journal of Propulsion and Power* 32.3 (2016), pp. 687–697. DOI: 10.2514/1.B35887.

[12] Cristian H Birzer and Con J Doolan. “Quasi-one-dimensional model of hydrogen-fueled scramjet combustors”. In: *Journal of propulsion and power* 25.6 (2009), pp. 1220–1225.
[13] Bora O Cakir, Ali Can Ispir, and Bayindir H Saracoglu. “Reduced order design and investigation of intakes for high speed propulsion systems”. In: *Acta Astronautica* (2022). DOI: 10.1016/j.actaastro.2022.07.037.
[14] Wei Huang. “Design exploration of three-dimensional transverse jet in a supersonic crossflow based on data mining and multi-objective design optimization approaches”. In: *international journal of hydrogen energy* 39.8 (2014), pp. 3914–3925. DOI: 10.1016/j.ijhydene.2013.12.129.
[15] Gianmarco Aversano et al. “PCA and Kriging for the efficient exploration of consistency regions in Uncertainty Quantification”. In: *Proceedings of the Combustion Institute* 37.4 (2019), pp. 4461–4469. DOI: 10.1016/j.proci.2018.07.040.
[16] Donald Stephen Gipe. “Surrogate Modelling of Combustion Systems for Robust Optimized Scramjet Design”. In: (2012).
[17] Wei Huang et al. “Performance evaluation and parametric analysis on cantilevered ramp injector in supersonic flows”. In: *Acta Astronautica* 84 (2013), pp. 141–152. DOI: j.actaastro.2012.11.011.
[18] Pietro Roncioni et al. “Numerical simulations and performance assessment of a scramjet powered cruise vehicle at Mach 8”. In: *Aerospace Science and Technology* 42 (2015), pp. 218–228. DOI: 10.1016/j.ast.2015.01.006.
[19] Gautam Choubey et al. “Numerical investigation on mixing improvement mechanism of transverse injection based scramjet combustor”. In: *Acta Astronautica* 188 (2021), pp. 426–437. DOI: 10.1016/j.actaastro.2021.08.008.
[20] S Chakravarthy et al. “Peroomian, 0”. In: *CFD++ User Manual, Version* 96 ().
[21] UDF Manual. “ANSYS FLUENT 12.0”. In: *Theory Guide* (2009).
[22] Ishmail B Celik et al. “Procedure for estimation and reporting of uncertainty due to discretization in CFD applications”. In: *Journal of Fluids Engineering* 130.7 (2008). DOI: 10.1115/1.2960953.
[23] Laura Painton Swiler and Gregory Dane Wyss. *A user’s guide to Sandia’s latin hypercube sampling software: LHS UNIX library/standalone version.* Tech. rep. Citeseer, 2004.
[24] François Chollet et al. *Keras*. https://keras.io. 2015.
[25] Kurt Hornik, Maxwell Stinchcombe, and Halbert White. “Multilayer feedforward networks are universal approximators”. In: *Neural networks* 2.5 (1989), pp. 359–366.
[26] James Bergstra and Yoshua Bengio. “Random search for hyper-parameter optimization”. In: *Journal of Machine Learning Research* 13.2 (2012).
[27] Kamila Zdybał et al. “Cost function for low-dimensional manifold topology assessment”. In: *manuscript submitted to Scientific Reports* (2022). DOI: 10.13140/RG.2.2.12370.84164.
[28] Kamila Zdybał et al. “PCAfold: Python software to generate, analyze and improve PCA-derived low-dimensional manifolds”. In: *SoftwareX* 12 (2020), p. 100630. DOI: 10.1016/j.softx.2020.100630.